Biophysical Journal Volume 86 April 2004 2455–2466



# High Metal Concentrations Are Required for Self-Association of Synaptotagmin II

Ricardo A. García* and Hilary Arnold Godwin*†

*Department of Biochemistry, Molecular Biology, and Cell Biology, and †Department of Chemistry, Northwestern University, Evanston, Illinois

ABSTRACT Several members of the synaptotagmin (syt) family of vesicle proteins have been proposed to act as $Ca^{2+}$ sensors on synaptic vesicles. The mechanism by which calcium activates this class of proteins has been the subject of controversy, yet relatively few detailed biophysical studies have been reported on how isoforms other than syt I respond to divalent metal ions. Here, we report a series of studies on the response of syt II to a wide range of metal ions. Analytical ultracentrifugation studies demonstrate that $Ca^{2+}$ induces protein dimerization upon exposure to 5 mM $Ca^{2+}$. Whereas $Ba^{2+}$, $Mg^{2+}$, or $Sr^{2+}$ do not potentiate self-association as strongly as $Ca^{2+}$, $Pb^{2+}$ triggers self-association of syt II at concentrations as low as 10 $\mu$M. Partial proteolysis studies suggest that the various divalent metals cause different changes in the conformation of the protein. The high calcium concentrations required for self-association of syt II suggest that the oligomerized state of this protein is not a critical intermediate in vesicle fusion; however, low-affinity calcium sites on syt II may play a critical role in buffering calcium at the presynaptic active zone. In addition, the high propensity of lead to oligomerize syt II offers a possible molecular explanation for how lead interferes with calcium-evoked neurotransmitter release.

## INTRODUCTION

Calcium-triggered release of neurotransmitter from synaptic vesicles is a tightly regulated process involving a large number of proteins on the synaptic vesicle surface (Brunger, 2000; Fon and Edwards, 2001; Lin and Scheller, 2000; Misura et al., 2000; Mochida, 2000). Substantial efforts have been put forth to identify the $Ca^{2+}$ sensor(s) that mediate activation and fusion of synaptic vesicles with the presynaptic membrane. Strong evidence points to the synaptotagmin (syt) proteins as the primary receptors of the $Ca^{2+}$ signal on synaptic vesicles (Brose et al., 1992; Elferink et al., 1989; Fernandez-Chacon et al., 2001; Geppert et al., 1994; Perin et al., 1990; Reist et al., 1998). Despite numerous studies detailing the activities of the protein components of the fusion apparatus, the exact mechanism(s) by which $Ca^{2+}$ regulates the fusogenic activity of syt remains the subject of intense debate (Damer and Creutz, 1996; Davletov et al., 1998; Davletov and Sudhof, 1994; García et al., 2000; Osborne et al., 1999; Shao et al., 1997). Possible mechanisms of $Ca^{2+}$ activation include metal-mediated phospholipid/membrane binding/penetration (Bai et al., 2000; Chae et al., 1998; Chapman et al., 1998; Chapman and Jahn, 1994; Davis et al., 1999; Davletov et al., 1998, 1993; Li et al., 1995a; Perin et al., 1990; Schiavo et al., 1996; Shin et al., 2002; Sugita et al., 1996, 2002; Zhang et al., 1998), conformational changes (Davletov and Sudhof, 1994; García et al., 2000), binding to protein partners (Chapman et al., 1998, 1995; Leveque et al., 2000; Matos et al., 2000; Schiavo et al., 1996; Shao et al., 1997; Sugita and Sudhof, 2000; Verona et al., 2000; von Poser et al., 2000; Zhang et al., 1994), changes in electrostatics (Shao et al., 1997), phosphorylation (Verona et al., 2000), and/or oligomerization (Chapman et al., 1996, 1998; Damer and Creutz, 1996; Desai et al., 2000; Fukuda and Mikoshiba, 2000a,b; Littleton et al., 2001, 1999; Osborne et al., 1999; Sugita et al., 1996).

To date, 15 isoforms of syt have been identified in neuronal and nonneuronal tissues (Schiavo et al., 1998; Sudhof, 2002; von Poser and Sudhof, 2001; Fukuda 2003a,b), suggesting a more global role for syts in intracellular membrane transport. The observation that individual isoforms of syt are expressed at varied levels in different tissue types has led to the hypothesis that each syt isoform may exhibit a distinct $Ca^{2+}$ response and/or perform unique functions (Littleton et al., 2001, 1999; Osborne et al., 1999; Schiavo et al., 1998; Sudhof, 2002; Sugita et al., 2002; Sugita and Sudhof, 2000). Of all of the syt family members, syt I is the best-characterized isoform. Upon binding of $Ca^{2+}$, syt I binds to the SNARE (soluble *N*-ethylmaleimide-sensitive factor attachment protein receptor) complex (Chapman et al., 1995; Shao et al., 1997; Sugita and Sudhof, 2000) at the nerve terminal and triggers fusion of synaptic vesicles with the presynaptic membrane. Syt II (Fukuda and Mikoshiba, 2000c), originally identified by Sudhof and coworkers, shares a high degree of sequence homology with syt I, but exhibits different expression patterns (Mochly-Rosen et al., 1992). As is true for syt I, syt II spans the synaptic vesicle membrane once via an N-terminal transmembrane domain and contains two cytosolic $Ca^{2+}$-binding

*Submitted March 27, 2003, and accepted for publication September 22, 2003.*

Address reprint requests to Hilary Arnold Godwin, Dept. of Chemistry, Northwestern University, 2145 Sheridan Rd., Evanston IL 60208-3113. Tel.: 847-467-3543; Fax: 847-491-7713; E-mail: h-godwin@northwestern.edu.

*Abbreviations used*: syt, synaptotagmin; C2, a calcium-binding domain homologous to the second regulatory domain from protein kinase C; C2A and C2B, the first and second calcium-binding domains in synaptotagmin II, respectively; GST, glutathione-*S*-transferase; SNARE, soluble *N*-ethylmaleimide-sensitive factor attachment protein receptor; syn, syntaxin.



0006-3495/04/04/2455/12 $2.00

C2 domains (C2A and C2B). The C2 domains are each highly homologous with the C2 regulatory region of protein kinase C (Mochly-Rosen et al., 1992; Perin et al., 1990), the protein from which the term ''C2 domain'' was originally coined. C2 domains have subsequently been identified in over 130 proteins in signaling pathways (http://www.expasy.ch/cgi-bin/prosite-search-ac?PS50004), with functions ranging from phospholipid binding and $Ca^{2+}$ signaling to ubiquitination (Nalefski and Falke, 1996; Rizo and Sudhof, 1998).

Synaptotagmins exhibit a high degree of specificity in binding to target molecules. The C2A and C2B domains are each responsible for distinct binding interactions in both $Ca^{2+}$-dependent and $Ca^{2+}$-independent manners (Sugita et al., 1996). For syts I and II, the C2A domain binds negatively charged phospholipids (particularly phosphatidylserine) at low $Ca^{2+}$ concentrations (5–10 $\mu$M), and syntaxin (a member of the SNARE complex) at higher $Ca^{2+}$ concentrations (>200 $\mu$M) (Chae et al., 1998; Chapman et al., 1998; Davletov and Sudhof, 1993; Kee and Scheller, 1996; Sugita and Sudhof, 2000; Sutton et al., 1995; Verona et al., 2000; Zhang et al., 1998). It seems likely that $Ca^{2+}$ potentiates these binding events at least in part via an electrostatic switch mechanism (Davletov et al., 1998; Shao et al., 1997), where $Ca^{2+}$ binding to syt shields the negatively charged residues within the binding regions of the C2 domains and facilitates interactions with the negatively charged binding sites of target molecules such as proteins and phospholipids (Chae et al., 1998; Chapman and Jahn, 1994; Shao et al., 1997; Zhang et al., 1998). Fluorescence resonance energy transfer studies with syt I revealed that $Ca^{2+}$ binding triggers global changes in conformation via rearrangement of C2 domains that are driven by changes in electrostatic charge within each C2 domain (García et al., 2000). The C2A domain of syt I has also been shown to penetrate lipid bilayers upon exposure to $Ca^{2+}$, suggesting a more direct role of C2A in catalyzing membrane fusion (Bai et al., 2000; Chapman et al., 1998). Both C2 domains are necessary for high-affinity binding of syt I to syntaxin and to SNAP-25 (a member of the SNARE complex), although significant binding is maintained in the isolated C2A domain (Chapman et al., 1996; Gerona et al., 2000). The C2B domain of syt I binds to phosphoinositides in a strictly $Ca^{2+}$ dependent manner (Schiavo et al., 1998). Binding of C2B of syt I to the clathrin adaptor protein, AP-2 (Chapman et al., 1998; Zhang et al., 1994), and to SNAP-25 (Schiavo et al., 1998) occurs independent of $Ca^{2+}$. The C2B domain has also been implicated in mediating protein homo- and heterodimerization of various syt isoforms upon exposure to $Ca^{2+}$ (Chapman et al., 1996, 1998; Fukuda et al., 1999; Osborne et al., 1999; Sugita et al., 1996).

The propensity of syts to self-associate has led to the assertion that oligomerization of syt is a prerequisite for subsequent interactions with the SNARE complex, and is thus necessary for membrane fusion (Chapman et al., 1996, 1998; Damer and Creutz, 1996; Desai et al., 2000; Fukuda et al., 1999; Fukuda and Mikoshiba, 2000a, 2001; Littleton et al., 2001, 1999; Osborne et al., 1999; Sugita et al., 1996). However, for isoforms other than syt I, little is known about the metal dependence or metal specificity for triggering self-association, and no reports have been made about the extent toxic metal exposure can affect this process. The effect of toxic metals is of particular interest given the recent discovery that syt I is a target for $Pb^{2+}$ (Bouton et al., 2001). Given the high level of sequence identity between syt isoforms, other members of the family are likely to be targets for $Pb^{2+}$ as well. To address these issues, we have analyzed the association state of syt II in the presence of various divalent metal cations, including $Pb^{2+}$. In addition, we have further characterized the $Ca^{2+}$-activated state of syt II by assessing metal-induced conformational changes by partial proteolysis coupled with MALDI-TOF mass spectrometry.

## MATERIALS AND METHODS

### Preparation of recombinant syt II

The cDNA encoding mouse syt II (residues 1–422) was obtained from Dr. Mitsunori Fukuda (RIKEN, Brain Science Institute, Wako City, Saitama, Japan). The cytosolic domain of syt II (residues 104–422), C2A (residues 104–267), and C2B (residues 262–422) were polymerase chain reaction (PCR) amplified using PCR primers that contained restriction sites for *Bam*HI (5′) and *Eco*RI (3′). The PCR-derived DNA was digested by *Bam*HI and *Eco*RI endonucleases to create compatible ends for insertion into the GST-expression vector pGEX-PKT (Sehgal et al., 2000) at these restriction sites. Successful insertion of the gene was verified by restriction analysis, DNA sequencing, and SDS-polyacrylamide gel electrophoresis (SDS-PAGE) of the protein products. The GST-fusion proteins were overexpressed in *Escherichia coli* BL21/DE3 cells and purified by affinity chromatography using glutathione-sepharose beads (Amersham Pharmacia, Amersham, UK). The GST moiety was removed by thrombin cleavage on the resin. Proteins were further purified by size-exclusion chromatography using a Superdex 75 column (Amersham Pharmacia). Fractions containing pure protein, as determined by SDS-PAGE, were dialyzed against 10 mM Bis-Tris, 100 mM KCl, 2 mM EDTA, pH 7.0, and then against 10 mM Bis-Tris, 100 mM KCl, pH 7.0. MALDI-TOF mass spectrometry was used to confirm that the proteins obtained were of the correct molecular mass: syt II (residues 104–422), predicted molecular weight = 36,079 mol wt, observed = 36,081 mol wt; C2A (residues 104–267), predicted molecular weight = 18,528 mol wt, observed = 18,532 mol wt; C2B (residues 262–422) predicted molecular weight = 18,313 mol wt, observed = 18,310 mol wt. The concentrations of standardized solutions of syt II (residues 104–422) were calibrated by amino acid analysis (Keck Biophysics Facility at Yale University, New Haven, CT) and used to calculate the extinction coefficient of the protein (43,980 $M^{-1}$ $cm^{-1}$). Protein concentrations of C2A and C2B were determined using the Bradford protein concentration assay (Bio-Rad, Hercules, CA).

### Analytical ultracentrifugation

Sedimentation equilibrium experiments were conducted using a Beckman XLA-70 analytical ultracentrifuge (Fullerton, CA). Syt II (residues 104–422) was centrifuged at protein concentrations of 2.5 $\mu$M and 7.5 $\mu$M and at rotor speeds of 19,000 and 22,000 rpm in a four-hole Beckman An60 Ti rotor cooled to 4°C. Samples were prepared in buffer (10 mM Bis-Tris, 100 mM KCl, pH 7.0) with either no divalent metal added, or in the presence of various concentrations of $CaCl_2$, $BaCl_2$, $MgCl_2$, and $SrCl_2$ (110 $\mu$M, 550 $\mu$M, 1.1 mM, 5 mM, 10 mM). Sedimentation equilibrium experi-

ments conducted in the presence of $Pb^{2+}$ were prepared in buffer (10 mM Bis-Tris, pH 7.0) with either no metal added, or in the presence of various concentrations of $Pb(NO_3)_2$ (10 $\mu$M, 50 $\mu$M, 110 $\mu$M, 550 $\mu$M, 1.1 mM). Parallel sedimentation equilibrium experiments were also performed with C2A (residues 104–267) and C2B (residues 262–422) at concentrations of 8.5 $\mu$M and 26 $\mu$M for C2A and 5 $\mu$M and 15 $\mu$M for C2B, and at rotor speeds of 27,000 and 32,000 rpm. Samples of C2A and C2B were prepared in buffer (10 mM Bis-Tris, 100 mM KCl, pH 7.0) with either no divalent metal added, or in the presence of various concentrations of $CaCl_2$ (110 $\mu$M, 550 $\mu$M, 1.1 mM, 5 mM, 10 mM). Attainment of equilibrium was assessed by analysis of difference plots of successive absorbance scans. Data taken at all speeds and all protein concentrations were fit simultaneously using a global fitting procedure to single-species or associative models. Data were analyzed using WinNonlin2 1.03 (http://spin3.mcb.uconn.edu/) and Sedntrp 1.01 (ftp://alpha.bbri.org/rasmb/spin/ms_dos/sedntrp-philo/) software. For the associative model, the theoretical molecular weight of monomeric syt II was input as a known value and the association constant was varied to obtain the best fit to the data. The association constants obtained in this manner reflect the net equilibrium for both the affinity of syt II for $Ca^{2+}$ and the affinity of $Ca^{2+}$-syt II for itself:

$$\text{monomer} + n\text{ca}^{2+} \overset{K_a(\text{Ca-syt})}{\rightleftharpoons} [(\text{Ca}^{2+})_n\text{monomer}] \times \overset{K_a(\text{syt-syt})}{\rightleftharpoons} [(\text{Ca}^{2+})_{2n}\text{dimer}].$$

In the absence of independent measures of the affinity of syt II for $Ca^{2+}$ ($K_a$(Ca-syt)), it is not possible to extract the value for the self-association of syt from the affinity constant obtained from the fit, except at the highest $Ca^{2+}$ concentrations (where all syt molecules are fully saturated with $Ca^{2+}$). Thus, to assess more quantitatively how $Ca^{2+}$ affects the self-association of syt II, the fraction of dimer was calculated from the apparent molecular weight obtained from the single ideal species fit ($MW_{observed}$) at each $Ca^{2+}$ concentration:

$$\frac{[\text{dimer}]}{[\text{total syt}]} = \frac{MW_{\text{observed}} - MW_{\text{monomer}}}{MW_{\text{dimer}}},$$

where $MW_{monomer}$ and $MW_{dimer}$ are the calculated molecular weights for syt II (residues 104–422) monomer (36,079 mol wt) and dimer (72,148 mol wt), respectively.

## Atomic force microscopy of syt II

Protein samples were analyzed in air with a Multimode atomic force microscope (AFM) (Digital Instruments, Santa Barbara, CA) operated in tapping mode using Digital Instruments n+ silicon nitride tapping mode probes with a force constant of $C = 40$–$100$ N/m and a resonance frequency of $n_o = 300$–$400$ kHz (García et al., 1996; Schneider et al., 1998). Samples of syt II (50–500 nM) were prepared in 20 $\mu$l of buffer (10 mM Bis-Tris, 100 mM KCl, pH7.0) with either no divalent metal added, or in the presence of 5 mM $CaCl_2$. Protein samples were incubated for ~5 min at 20°C. Samples were deposited onto freshly cleaved ruby mica (New York Mica, New York, NY), washed with 15–20 drops of deionized water, blotted with filter paper, and blown dry under a stream of $N_2$ gas. All samples were imaged at a scan rate of 2.2–3.2 lines/s (512 × 512 pixels per image). The force exerted on the sample was minimized by retracting the tip as far from the surface as possible without a loss of resolution in the images. All images were acquired without online filtering.

## AFM image analysis

Protein heights and diameters were measured from the unflattened images using the section analysis function of the Nanoscope III offline data analysis software (version 4.32r3; Digital Instruments). Proteins were measured at half-maximal height to compensate for the lateral broadening effects of AFM raster scanning (Schneider et al., 1998). Measurements of molecular volume of the scanned proteins were calculated from the height and diameter measurements as described previously (Schneider et al., 1998). The theoretical molecular volume of syt II was also calculated according to the method of Edstrom et al. (1990). Captured images were flattened to remove the background slope.

## Partial proteolysis of syt II

Proteolysis experiments were conducted with ~30 $\mu$M syt II and 4 $\mu$g of trypsin (Sigma, St. Louis, MO) in buffer (10 mM Bis-Tris, 100 mM KCl, pH 7.0) with either no divalent metal added, or in the presence of various concentrations of $CaCl_2$ (110 $\mu$M, 550 $\mu$M, 1.1 mM, 5 mM, 10 mM). Experiments designed to assess metal-specific conformational changes by trypsin proteolysis were conducted with either no divalent metal, or in the presence of 5 mM $CaCl_2$, $SrCl_2$, $BaCl_2$, $MgCl_2$, or 1.1 mM $Pb(NO_3)_2$. Samples were prepared in 20-$\mu$l volumes, gently vortexed, and incubated at 37°C for 1 h. Reactions were stopped by the addition of SDS-sample buffer (Laemmli, 1970) followed by boiling at 95°C and were analyzed by SDS-PAGE. Control experiments with 30 $\mu$M bovine serum albumin (Sigma) were conducted under identical conditions to those described for syt II with either no divalent metal, or in the presence 5 mM $CaCl_2$, $SrCl_2$, $BaCl_2$, or $MgCl_2$; or 1.1 mM $Pb(NO_3)_2$.

## MALDI-TOF mass spectrometry of syt II

Samples of intact syt II (residues 104–422) and trypsin-digested syt II (residues 104–422) were analyzed by MALDI-TOF mass spectrometry using a Voyager DE Pro spectrometer from PE Biosystems (Foster City, CA) operated in linear mode. The MALDI matrix was prepared by dissolving 10 mg of sinapinic acid (Sigma) in 1 ml of 50% acetonitrile in water. Samples of intact syt II were prepared by adding 1 $\mu$l of protein (80 $\mu$M) to 9 $\mu$l of matrix solution. Trypsin digests of syt II in the presence of 5 mM $CaCl_2$, $SrCl_2$, $BaCl_2$, $MgCl_2$, or 1.1 mM $Pb(NO_3)_2$ were prepared as described in the previous section and stopped after 1 hr by boiling the samples for 5 min at 95°C. The samples were briefly centrifuged and a 4-$\mu$l aliquot of each trypsin digest was added to 11 $\mu$l of matrix solution. All samples were briefly vortexed, spotted on a 100-well stainless steel sample plate (~1–2 $\mu$l of analyte per well), and allowed to air dry. MALDI-TOF mass spectra of all samples were collected in negative ion mode with delayed extraction (300 ns), and at an acceleration voltage of 25 kV. Internal and/or external mass calibrations were performed using bovine carbonic anhydrase II ($MW = 28{,}980$ mol wt) or horse heart cytochrome $c$ ($MW = 12{,}361$ mol wt) (Sigma). Fragment masses were compared to predicted cleavage products of syt II (residues 104–422) produced by trypsin cleavage using the MS Digest program on the ProteinProspector internet site (version 3.4.1; http://prospector.ucsf.edu/).

## Modeling of syt II

The coordinates of the crystal structure of syt III (Sutton et al., 1999) were downloaded from the Protein Data Bank (http://www.rcsb.org/pdb/cgi/explore.cgi?pid=25992988744610&pdbId=1DQV) and used as a scaffold for threading of the sequence comprising the cytosolic region of syt II (residues 104–422) using the Swiss-PdbViewer program (http://www.expasy.ch/spdbv/mainpage.html). The Swiss-PdbViewer was also used to align the cytosolic domains of syt II (residues 104–422) and syt III (residues 295–566) before threading the syt II amino acid sequence to the syt III scaffold.

# RESULTS

To determine the propensity of $Ca^{2+}$ to mediate self-association of syt II, sedimentation equilibrium experiments

were conducted on the full cytosolic domain of syt II (residues 104–422) in the absence of divalent metal, and in the presence of increasing concentrations of $Ca^{2+}$. These data were analyzed to determine the apparent molecular weight of syt II using a single ideal species model in the program WinNonlin2 (see Materials and Methods). The results of analyses for syt II are provided in tabular form in the supplemental materials (see Supplementary Material). In the absence of $Ca^{2+}$, the apparent molecular weight of syt II (37,300 mol wt) is consistent with the calculated molecular mass of the polypeptide (36,079 Da), indicating that the apo form of the protein is monomeric. A comparison of the equilibrium scans of syt II taken without divalent metal in the buffer, and in the presence of 550 $\mu$M and 5 mM $Ca^{2+}$ reveals a dramatic shift in the absorbance profiles (Fig. 1): at higher $Ca^{2+}$ concentrations, the absorbance increases more dramatically as a function of increasing cell radius. Fits to these data using a single ideal species model reveal that increasing the $Ca^{2+}$ concentration results in a corresponding increase in molecular weight (see supplemental materials). The fraction of dimer observed as a function of $Ca^{2+}$ concentration is plotted in Fig. 2. From the plot, the $EC_{50}$ for dimerization occurs at ~1 mM $Ca^2$. Complete formation of a protein dimer (calculated $MW = 72{,}158$; observed $MW = 75{,}100$ mol wt) is observed at 5mM $Ca^{2+}$. At the concentration at which syt II is saturated with $Ca^{2+}$ (5 mM $CaCl_2$), the associative model yields a dissociation constant for the dimer of 0.5 $\mu$M.

To determine whether self-association of syt II is specifically mediated by $Ca^{2+}$, parallel sedimentation equilibrium experiments were also conducted with $Ba^{2+}$, $Mg^{2+}$, $Sr^{2+}$, and $Pb^{2+}$ and analyzed using a single ideal

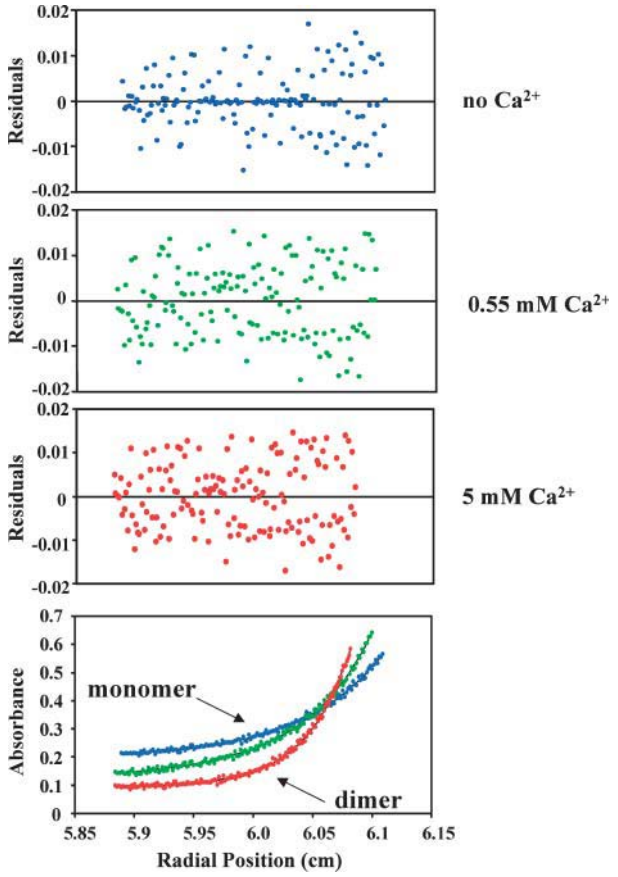


FIGURE 1 Sedimentation equilibrium analysis of syt II. Samples of syt II (2.5 and 7.5 $\mu$M) were centrifuged at two speeds (19,000 and 22,000 rpm) as described in Materials and Methods. For clarity, only the absorbance scans taken at 22,000 rpm are shown. Absorbance scans of syt II taken at equilibrium in the absence of divalent metal (*blue trace*) and in the presence of 0.55 mM (*green trace*) or 5 mM $Ca^{2+}$ (*red trace*) are shown in the bottom panel and the corresponding residuals are displayed above. The transition from monomer (*blue trace*) to dimer (*red trace*) correlates with the increase in $Ca^{2+}$ concentration.

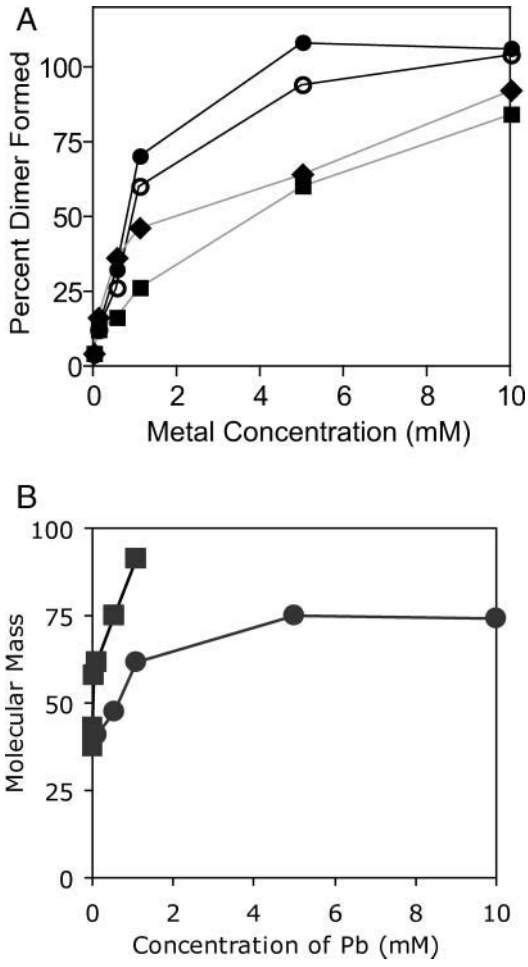


FIGURE 2 Comparative plot of percent syt II oligomerization state as a function of divalent metal concentration. (*A*) The percent dimer present at different metal concentrations was calculated from the molecular weights obtained from a single ideal species fit to the sedimentation equilibrium data. Essentially 100% dimer is present at a $Ca^{2+}$ concentration (●) of 5 mM; $Sr^{2+}$ (○) promotes dimer formation almost as well as $Ca^{2+}$. By contrast, $Mg^{2+}$ (♦) and $Ba^{2+}$ (■) are much weaker promoters of dimer formation, and even 10 mM $Mg^{2+}$ or $Ba^{2+}$ does not yield 100% protein dimer. (*B*) $Pb^{2+}$ (■) is a more potent mediator of self-association than $Ca^{2+}$ (●); complete dimer formation is seen at 1 mM $Pb^{2+}$.

species model as described above. Exposure of syt II to increasing concentrations of each of these metals gives rise to metal-dependent protein self-association (see Table S1, *B–E*, in supplemental materials). Comparison of the degree of dimer formation as a function of divalent metal concentration reveals that $Ba^{2+}$ and $Mg^{2+}$ are significantly less potent mediators of self-association than $Ca^{2+}$ and that very high concentrations of $Sr^{2+}$ (~10 mM) are required to achieve complete formation of syt II dimer (Fig. 2 *A*). Similar sedimentation equilibrium experiments conducted in the presence of $Pb^{2+}$ were performed at a lower range of metal concentration (0–1.1 mM) because protein precipitated at $Pb^{2+}$ concentrations above 1.1 mM. Exposure of syt II to $Pb^{2+}$ triggered protein self-association at $Pb^{2+}$ concentrations as low as 10 $\mu$M and yielded complete formation of protein dimer at 1 mM $Pb^{2+}$ (Fig. 2 *B*).

To identify whether a particular domain of syt II is responsible for self-association, sedimentation equilibrium experiments were also performed with isolated C2A and C2B domains and analyzed as described above using a single ideal species model. The results of these fits for C2A and C2B are given in Table S2 of the supplemental materials. Sedimentation equilibrium results (19.1–21.6 kDa) for C2A (residues 104–267) indicate that the domain is predominantly monomeric, even when exposed to increasing $Ca^{2+}$ concentrations (see Fig. 3). Parallel experiments conducted with the isolated C2B domain (residues 262–422) indicate that C2B also exists as a monomer (17.5–19.7 kDa), irrespective of $Ca^{2+}$ concentration (0–10 mM). These results show that neither C2A nor C2B independently has a propensity for self-association and suggest that both domains and/or an intact linker between domains are required for $Ca^{2+}$-triggered association of C2A-C2B cytosolic region of syt II.

Calcium-mediated self-association of syt II was also investigated by AFM. Samples of syt II were adsorbed onto freshly cleaved ruby mica with either no divalent metal added, or in the presence of 5 mM $Ca^{2+}$, and scanned in air. Fig. 4, *A* and *B*, show representative images of syt II molecules in the absence and presence of $Ca^{2+}$, respectively. The dimensions of protein molecules analyzed from several such images were performed using the methods previously described by Schneider et al. (1998); see also Table 1 in this article. To compare the behavior of apo and $Ca^{2+}$-exposed syt II quantitatively, the apparent molecular volumes of proteins from the AFM images were determined, as well as the theoretical molecular volumes of monomeric and dimeric syt II (Edstrom et al., 1990; Schneider et al., 1998). The average apparent molecular volume calculated for syt II in the absence of divalent metal (28 ± 11 $nm^3$) increased upon exposure to 5 mM $Ca^{2+}$ (120 ± 33 $nm^3$). The molecular volume measured for syt II in the presence of $Ca^{2+}$ approximates the theoretical value calculated for a dimer (136.8 $nm^3$; Edstrom et al., 1990). However, in the absence of $Ca^{2+}$ the average molecular volume measured (28 ± 11 $nm^3$) is markedly lower than that predicted for the apo-protein by the theoretical model (68.4 $nm^3$). The low molecular volume observed for apo-syt II presumably arises because the apo-protein molecules are more susceptible to tip-induced deformation effects that reduce the apparent heights, which is consistent with previous studies that revealed that isolated C2 domains of syt are less stable without $Ca^{2+}$ (Shao et al., 1997; Smith and Augustine 1988). Overall, the results by AFM are consistent with a model in which $Ca^{2+}$ mediates self-association of syt II, causing the protein to undergo a transformation from a small monomeric apo form to a large dimeric (or oligomeric) form at high $Ca^{2+}$ concentrations.

Because previous studies suggested that $Ca^{2+}$ induces a conformational change in syt I (Bouton et al., 2001; Davletov et al., 1998; García et al., 2000), partial proteolysis experiments were conducted on syt II to determine the effects of $Ca^{2+}$ binding on the conformation of the protein.

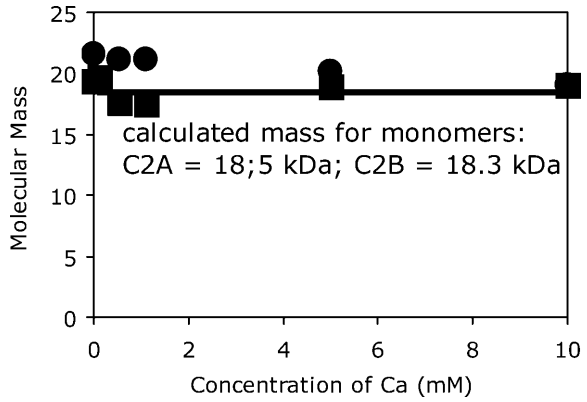


FIGURE 3 Association state of individual C2 domains from syt II as a function of calcium concentration. The observed molecular mass for isolated C2A (●) and C2B (■) are close to the calculated masses for the monomers (18.5 kDa and 18.3 kDa, respectively) and remain constant as a function of added calcium, suggesting that the isolated domains are not oligomerization competent.

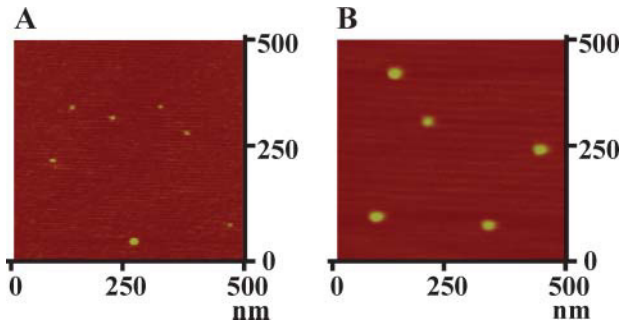


FIGURE 4 AFM images of syt II in air. Individual protein molecules of syt II (*A*) without $Ca^{2+}$ and (*B*) with 5 mM $Ca^{2+}$ are shown. Addition of $Ca^{2+}$ to the protein samples increases the size dimensions of the molecules (see Table 1). Proteins for analysis were visualized at 800–3000-nm scan sizes. For comparisons, representative images were magnified to 500 nm × 500 nm.

**TABLE 1 Size dimensions of syt II measured using atomic force microscopy in the absence and presence of $Ca^{2+}$**

| Sample | *n* | Diameter at half-height (nm) | Height (nm) | $V_m$ ($nm^3$) | $V_c$ ($nm^3$) |
|---|---|---|---|---|---|
| syt II-apo | 37 | 18.7 ± 3.2 | 0.54 ± 0.25 | 28.0 ± 12 | 68.4 |
| syt II + 5 mM $Ca^{2+}$ | 41 | 36.3 ± 4.0 | 0.73 ± 0.16 | 120 ± 33 | 136.8 |

The volume measured for syt II by AFM (*V*m) was determined for a population of protein molecules (*n*) deposited onto mica and compared to the theoretical volume calculated (*V*c) for the monomeric and dimeric forms of the protein.

In these experiments, changes in the degree and/or site selectivity of protease cleavage within the target protein as a function of ligand binding are indicative of alterations in protein structure (Davletov and Sudhof, 1994). A change in the proteolytic pattern could arise from three possible events: a simple dimerization (or oligomerization) event, a dimerization-independent conformational (or dynamic) change, or a more complex conformational/dynamic change in the structure of the individual subunits that occurs concomitant with dimerization. Changes in the proteolytic accessibility of the cytosolic domain of syt II as a function of $Ca^{2+}$ concentration were analyzed using trypsin (Fig. 5). In the absence of trypsin, syt II remains intact as indicated by SDS-PAGE (lane −T). Addition of trypsin to the samples triggers cleavage of the protein. The degree and pattern of proteolysis is almost identical in samples containing 0–1.1 mM $Ca^{2+}$: ~98% of the intact protein is proteolyzed by trypsin and two major tryptic fragments are the end products of the cleavage reaction. (Under high protein-loading conditions, a band corresponding to trypsin is also visible; see Fig. 6). By contrast, extensive protection of the intact protein band is observed at $Ca^{2+}$ concentrations of 5 and 10 mM (Fig. 5). As a control, trypsin proteolysis experiments were also conducted on bovine serum albumin (data not shown) under identical conditions as those described for syt II. The results demonstrated that the efficiency of trypsin cleavage of bovine serum albumin is slightly increased as a function of increasing $Ca^{2+}$ concentration, which is completely opposite the trend observed with syt II. These data suggest that the $Ca^{2+}$-dependent change in the degree of proteolysis of syt II reflects a change in the accessibility of the cleavage sites in the protein, and are not simply due to $Ca^{2+}$-dependent changes in the activity of trypsin. Taken together with the analytical ultracentrifugation and AFM data presented herein, these results suggest that $Ca^{2+}$ triggers a structural change in syt II that arises at the same high $Ca^{2+}$ concentrations that induce dimerization.

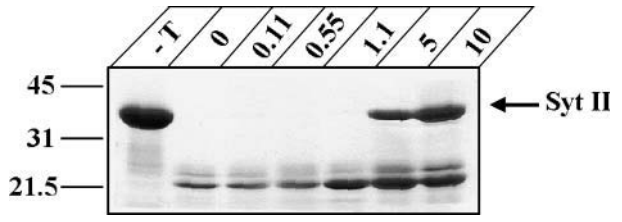


FIGURE 5 Calcium-dependent protease protection of syt II. Proteolysis experiments were carried out with ~30 μM syt II and 2 μg of trypsin in the absence (lane 0) and presence of increasing millimolar concentrations of $Ca^{2+}$ (lanes 0.11, 0.55, 1.1, 5, 10). Control lane (−T) shows syt II (denoted by the *arrow*) without treatment with trypsin. Protein products were analyzed by SDS-PAGE and observed by Coomassie blue staining. Molecular weight markers are shown on the left.

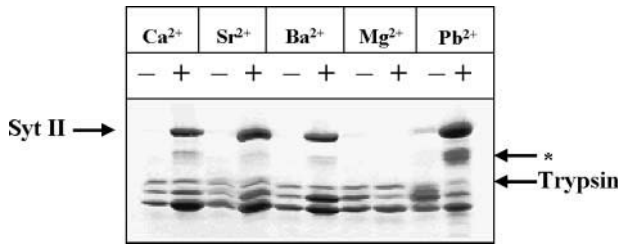


FIGURE 6 Metal-specific protease protection of syt II. Proteolysis experiments were carried out with ~30 uM syt II and 2 μg of trypsin in the absence (−) and presence (+) of 5 mM $Ca^{2+}$, $Sr^{2+}$, $Ba^{2+}$, $Mg^{2+}$,or 1.1 mM $Pb^{2+}$. Intact syt II is denoted by the arrow. Trypsin cleavage in the presence of $Pb^{2+}$ gives rise to a distinct proteolytic fragment below the intact syt II band (denoted by the *asterisk*). Protein products were analyzed by SDS-PAGE and observed by Coomassie blue staining.

To determine whether the metal-triggered conformational change observed by proteolysis arises solely from protein dimerization or are independent of dimerization, parallel trypsin digests were also conducted in the presence of 5 mM $Ba^{2+}$, $Mg^{2+}$, $Sr^{2+}$, or 1.1 mM $Pb^{2+}$ (Fig. 6). Interestingly, the proteolysis patterns observed do not appear to correlate directly with the ability of a given metal ion to promote dimerization. Extensive protease protection of the full cytosolic domain of syt II occurs with 5mM $Ba^{2+}$, 5 mM $Sr^{2+}$, or 1.1 mM $Pb^{2+}$. By contrast, the cleavage pattern obtained in the presence of 5 mM $Mg^{2+}$—which promotes dimerization with roughly the same ability as 5 mM $Ba^{2+}$ (see Fig. 2)—resembles that obtained in the absence of divalent metal. The most pronounced degree of protease protection was mediated by $Pb^{2+}$ (Fig. 6). The similarity in cleavage patterns obtained with $Ca^{2+}$, $Ba^{2+}$, and $Sr^{2+}$ suggests that each of these metals induces a similar conformational change (or change in rigidity) in syt II. By contrast, the similarity in cleavage patterns obtained in the absence of divalent metal or in the presence of $Mg^{2+}$ suggest that syt II adopts an apo-like conformation in the presence of $Mg^{2+}$ that is distinct from that obtained with $Ca^{2+}$, $Ba^{2+}$, and $Sr^{2+}$. Lead also appears to induce a conformation that is different from that of $Ca^{2+}$: there is also a higher molecular weight fragment that is more stable in the presence of $Pb^{2+}$ than in the presence of the other metal ions (Fig. 6, denoted by the *asterisk*). Alterations in trypsin activity by these metals was ruled out by conducting trypsin cleavage experiments performed with bovine serum albumin under

identical conditions as those described here (5 mM $Ca^{2+}$, $Ba^{2+}$, $Sr^{2+}$, $Mg^{2+}$, and 1.1 mM $Pb^{2+}$: data not shown); additional cleavage of BSA in the presence of these $Pb^{2+}$ was only observed at longer proteolysis reaction times than were used for the syt II experiments. Taken together, these studies suggest that, although dimerization of syt II is associated with a concomitant conformational change in the presence of $Ca^{2+}$, there is not necessarily a one-to-one correlation between the ability of a metal ion to promote dimerization and to induce the active conformation of the protein.

To further characterize the nature of the conformational change(s) induced by addition of divalent metal ions to syt II, molecular weights of the protein fragments derived from the trypsin digests were determined using MALDI-TOF mass spectrometry and the cleavage sites of the fragments were mapped using the program MS Digest (Table 2). The MALDI-TOF mass spectrum of syt II in the absence of both trypsin and divalent metal reveals a peak at the molecular weight of the monomeric protein (Fig. 7, *top panel*; Table 2). Trypsin digestion in the absence of metal or in the presence of $Mg^{2+}$ results in two protease-resistant fragments (F1 = 17,730 ± 11 mol wt; F2 = 18,742 ± 8 mol wt). Consistent with the results seen by SDS-PAGE, no peak corresponding to intact monomer is observed in either of these cases. The masses of F1 and F2 correspond to major segments of the C2A and C2B domains, respectively (Fig. 7, *second* and *third panels*; Table 2). By contrast, when $Ca^{2+}$ (or $Ba^{2+}$ or $Sr^{2+}$, data not shown) is present during the digestion, intact syt II (Fig. 7, *fourth panel*; Table 2) is observed in addition to the two protease-resistant fragments observed for the apo protein. In the presence of $Pb^{2+}$, only one of the protease-resistant fragments is present (F1), along with intact syt II (Fig. 5, *bottom panel*; Table 2). It is not clear why the additional proteolytic fragment observed by SDS-PAGE for the trypsin digest of the $Pb^{2+}$-exposed sample (Fig. 6; band highlighted by *asterisk*) is undetectable by mass spectrometry; presumably this fragment does not ionize or desorb efficiently in the mass spectrometer. Comparison of the relative intensities of the tryptic fragments (F1, F2, and intact syt II) in the $Ca^{2+}$- and $Pb^{2+}$-exposed samples reveal that the amount of the specific proteolytic fragments produced is dependent on the specific divalent metal present in the proteolysis reaction (Fig. 7).

Assignment of the significant cleavage sites within the protein was determined using the program MS Digest (version 3.4.1; http://prospector.ucsf.edu/) (Table 2). The cleavage sites were then located on a three-dimensional structure of syt II obtained by threading the sequence of syt II onto the known structure of syt III (Sutton et al., 1999) (Fig. 8). As was surmised from the molecular weights of the fragments, the detailed analysis suggests that the major fragments, F1 and F2, correspond roughly to the C2A and C2B domains, respectively. A significant cleavage site is present at Lys-273, which is located within the linker that separates the C2A and C2B domains. Trypsin cleavage within the linker at Lys-273 and at Lys-115 gives rise to a fragment composed mostly of the C2A domain. The cleavage site at Lys-115 resides in the N-terminal region that precedes the C2 domains of syt II: this region was not resolved in the structure of syt III. Independent cleavage within the C2A domain at Lys-223 and at the C-terminal region of syt II at Arg-389 results in a fragment composed mostly of the C2B domain.

## DISCUSSION

The data reported here demonstrate that high concentrations of $Ca^{2+}$ are required to trigger self-association of the cytosolic domain of syt II in the absence of any membrane components. Analyses of self-association of each isolated C2A and C2B domain of syt II indicate that each domain remains approximately monomeric, even in the presence of high concentrations of $Ca^{2+}$ (see Table S1 in the supplemental materials). The ability of syt II, but not the individual C2 domains, to self-associate in response to $Ca^{2+}$ indicates that the self-association process requires the presence of both C2A and C2B, and/or other functional regions within the cytosolic domain of syt II for precise regulation of the protein's fusogenic activity. The concentration of $Ca^{2+}$ required for complete dimer formation of syt II is significantly higher than recent measurements of $Ca^{2+}$ at the neuronal active zone during vesicle exocytosis, which range between 1 and 10 $\mu$M (Bollmann et al., 2000; Schneggenburger and Neher, 2000). However, given that syts I and II are found on the same synaptic vesicles (Osborne et al., 1999) and syt I has been found to colocalize with $Ca^{2+}$channels (Chapman et al., 1998), these low-affinity calcium sites on syt II may play an important

**TABLE 2 Molecular weights of the major proteolytic fragments of syt II as determined by MALDI-TOF mass spectrometry**

| Proteolytic fragment | Assignment (residues) | Calculated mass (Da) | Observed MW (mol wt) | | | | | |
|---|---|---|---|---|---|---|---|---|
| | | | apo | $Ca^{2+}$ | $Ba^{2+}$ | $Mg^{2+}$ | $Sr^{2+}$ | $Pb^{2+}$ |
| F1 | 116–273 | 17,745 | 17,750 ± 10 | 17,735 ± 5 | 17,730 ± 4 | 17,730 ± 11 | 17,721 ± 7 | 17,736 ± 3 |
| F2 | 224–389 | 18,766 | 18,755 ± 11 | 18,755 ± 5 | 18,747 ± 5 | 18,742 ± 8 | 18,734 ± 9 | – |
| Monomer′ | 113–420 | 34,687 | – | 34,751 ± 121 | 34,726 ± 130 | – | 34,661 ± 134 | – |
| Monomer′ | 116–422 | 34,555 | – | – | – | – | – | 34,553 ± 15 |

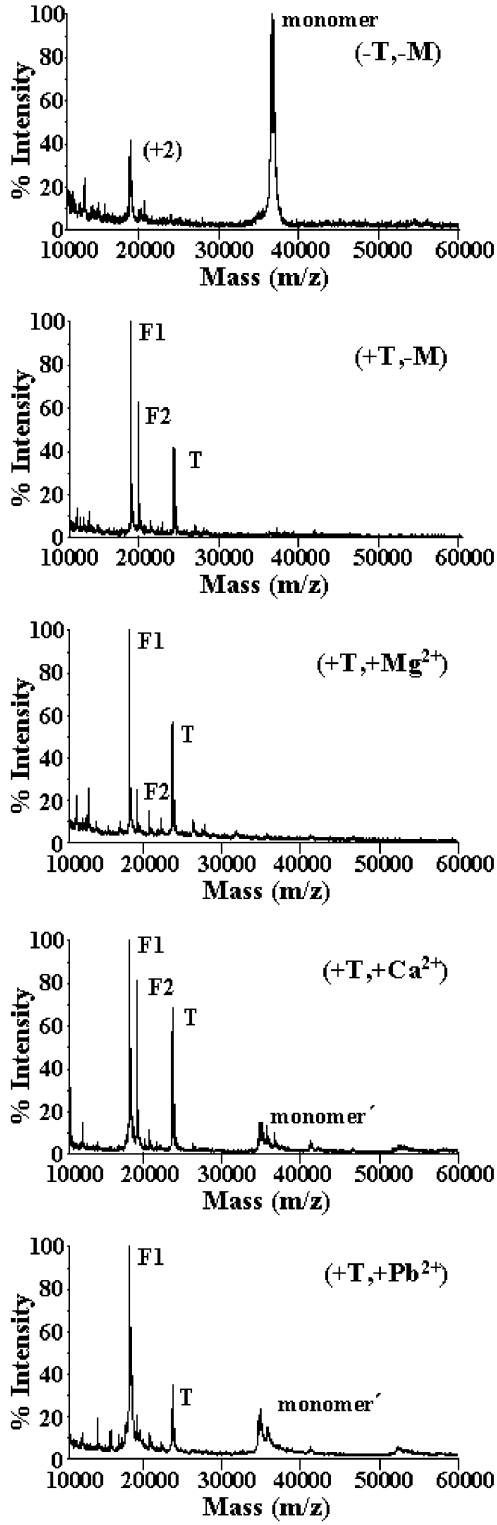


FIGURE 7 Identification of major proteolytic fragments of syt II. MALDI-TOF mass spectrum of apo-syt II in the absence of trypsin (−T,−M) reveals a peak at the molecular weight of the intact monomer (36,079 mol wt), and a less intense peak corresponding to its doubly protonated form (+2). Trypsin-digested samples in the absence of divalent metal (+T,−M), and in the presence of magnesium (+T,+$Mg^{2+}$), calcium (+T,+$Ca^{2+}$), and lead (+T, +$Pb^{2+}$) reveal the major protease-resistant polypeptide fragments (F1, F2) and the remaining intact protein (monomer′). The molecular weights of the various fragments are given in Table 2.

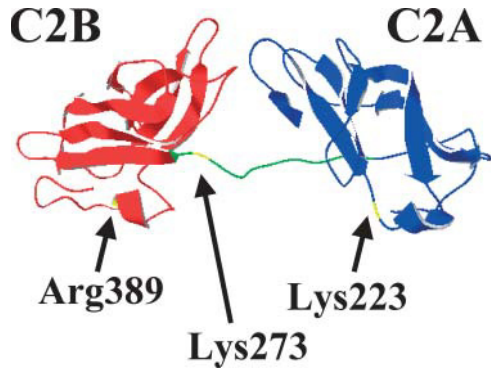


FIGURE 8 Modeled structure of syt II. Ribbon diagram of the modeled structure of syt II (residues 104–422) depicting the significant trypsin cleavage sites (*yellow*) contained within the C2A (*blue*) and C2B (*red*) domains, and also within the linker region separating C2A and C2B (*green*). Significant trypsin cleavage also occurs at Lys-115 (not shown).

role in calcium buffering at the presynaptic active zone (Felmy et al., 2003; Trommershèauser et al., 2003). Furthermore, it is possible that self-association of syt II occurs at lower calcium concentrations when membrane components are present.

It is interesting to compare these results for the cytosolic domain of syt II (residues 104–422) to those obtained previously from our laboratory (García et al., 2000) and by others (Chapman et al., 1996, 1998; Damer and Creutz, 1996; Desai et al., 2000; Fukuda and Mikoshiba, 2000b; Littleton et al., 2001, 1999; Osborne et al., 1999; Sugita et al., 1996) for syt I and other syt isoforms. In our hands, the cytosolic domain from syt I (residues 96–421) remains monomeric even when it is expressed, purified, and exposed to divalent cation, and analyzed (by analytical ultracentrifugation) in a manner identical to the conditions used herein to study syt II (García et al., 2000). Comparison of these data would suggest that there is something inherently different about oligomerization propensity between syt I and syt II, despite the high sequence identity (~82%) of the cytosolic domains of the two isoforms. However, several other groups have reported that syt I—and other syt family members—oligomerize either constitutively or in the presence of $Ca^{2+}$ (Chapman et al., 1996, 1998; Damer and Creutz, 1996; Desai et al., 2000; Fukuda and Mikoshiba, 2000b; Littleton et al., 2001, 1999; Osborne et al., 1999; Sugita et al., 1996). Furthermore, whereas some of these authors have found the oligomerization activity of syt to reside in the C2B domain (Chapman et al., 1996, 1998; Desai et al., 2000; Littleton et al., 2001), we find that C2B from syt II is monomeric even in the presence of high concentrations of $Ca^{2+}$.

How can these conflicting data be reconciled? Several possibilities must be considered:

Specific regions of syt (e.g., the transmembrane domain, Fukuda and Mikoshiba, 2000b; C2B, Chapman et al., 1996) are required for oligomerization; the different results observed in different laboratories arise from the use of proteins of different lengths.

Specific mutations (e.g., G374 versus D374) or polymorphisms present in syt isoforms used by different members of the community determine whether syt is able to oligomerize (Davis et al., 1999).

''Contaminants'' (Fernandez et al., 2001), membrane components, or posttranslational modifications (or the lack thereof; Fukuda and Mikoshiba, 2000b) are responsible for the propensity of syt to oligomerize; differences in purification protocols may account for the differences in oligomerization observed in different laboratories.

The ability of syts to oligomerize may be transient and hence lost with aging.

The data reported herein provide the following insights into these issues:

The transmembrane domain is not required for oligomerization. In addition to the data reported herein demonstrating that the cytosolic domain for syt II oligomerizes in response to $Ca^{2+}$. Fukuda and coworkers have also observed oligomerization of cytosolic domains (or portions thereof) for various syt isoforms (Fukuda and Mikoshiba, 2000b).

Although C2B may be necessary for oligomerization, it is not sufficient. No oligomerization was observed for isolated C2B from syt II (residues 262–422).

The presence of a glycine (instead of glutamate) at position 374 (syt I numbering) is not sufficient to confer the ability to oligomerize to syt. Both syt I (residues 96–421) (García et al., 2000) and syt II (residues 104–422) studied in our laboratory have glycine at this position, yet only syt II was observed to oligomerize.

Contaminants are not solely responsible for the $Ca^{2+}$-triggered oligomerization of syt II: all samples used herein were subjected to purification by gel filtration after isolation using affinity chromatography. No contaminants were observed by ultraviolet-visible (any samples with significant absorbance at 260 nm were rejected and not subjected to further analysis) or by mass spectrometry (syt II (residues 104–422), predicted molecular weight = 36,079 mol wt, observed = 36,081 mol wt). Clearly, parallel studies in the presence of membrane components are warranted, but these studies reveal that oligomerization occurs even in their absence.

The different behaviors that we observe for syt I and syt II, when isolated and studied under identical conditions, point to the clear need for detailed structural studies on these isoforms and mutagenesis studies that explore the role of specific residues in promoting oligomerization. Furthermore, studies on oligomerization of syt I and II under conditions that allow membrane association would also be of interest.

The studies reported herein also provide important insights into the metal dependence and specificity for self-association of syt II. Barium and magnesium are much weaker than $Ca^{2+}$ at triggering dimer formation of syt II (Fig. 2 *A*). These data are consistent with oligomerization studies performed by Chapman and co-workers with GST-immobilized cytosolic syt I that showed complex formation with native syt I in the presence of $Ca^{2+}$, but not with $Ba^{2+}$ or $Mg^{2+}$ (Chapman et al., 1996). By contrast, syt II self-associates in response to $Sr^{2+}$ in a manner similar to that of $Ca^{2+}$ (Fig. 2 *A*; Table S1D in the supplemental materials), although slightly higher concentrations of $Sr^{2+}$ ($\sim$10 mM) are required to yield complete dimer formation. This result is somewhat surprising, given that $Sr^{2+}$ does not trigger binding of syt II to syntaxin (Li et al., 1995b) and does not promote oligomerization of syt I (Chapman et al., 1996). Several possible explanations for these discrepancies must be considered: oligomerization of syt may not be a determinant (or the sole determinant) of activity; activation of syt II may not necessarily result in syntaxin binding; the different conditions used for different studies in different groups may account for the differences in observed behaviors; and/or syt II exhibits significantly different cation selectivities than syt I.

The ability of $Pb^{2+}$ to trigger oligomerization of syt II is of particular interest, given recent studies that suggest syts may be a target for $Pb^{2+}$ (Bouton et al., 2001). The propensity of $Pb^{2+}$ to trigger dimerization of syt II at a concentration approximately one order of magnitude less than that observed with $Ca^{2+}$ (550 $\mu$M $Pb^{2+}$ vs. 5 mM $Ca^{2+}$) indicates that $Pb^{2+}$ is a more potent mediator of the self-association process than $Ca^{2+}$. Exposure of syt II to $Pb^{2+}$ triggered protein self-association at $Pb^{2+}$ concentrations as low as 10 $\mu$M and yielded a multimeric species at 1.1 mM $Pb^{2+}$. By contrast, previous studies with syt I demonstrate that $Pb^{2+}$ is a potent substitute for $Ca^{2+}$ in potentiating interactions between syt I and phospholipid liposomes but that $Pb^{2+}$ interferes with the ability of syt I to bind to syntaxin (Bouton et al., 2001). Taken together, these results suggest that syts, as a class of proteins, may be important protein targets by which $Pb^{2+}$ mediates its neurotoxicity and that the differences between how $Pb^{2+}$ and $Ca^{2+}$ interact with different syt isoforms may explain why $Pb^{2+}$ inhibits the $Ca^{2+}$-evoked step of neurotransmitter release and increases spontaneous release (Manalis et al., 1984).

Critically, the studies reported herein demonstrate that divalent metals also induce a structural change in the protein that does not necessarily occur concomitant with dimerization. In the absence of metal, significant cleavage occurs within the linker region at Lys-273, which separates the C2A and C2B domains, and within C2A (Lys-223) and C2B (Arg-389). Protection from digestion occurs upon binding of $Ca^{2+}$

(5 mM), $Ba^{2+}$ (5 mM), $Sr^{2+}$ (5 mM), and $Pb^{2+}$ (1 mM), due to a change in the structure or dynamics of syt II that renders the cleavage sites inaccessible to the protease. However, even though $Mg^{2+}$ promotes dimer formation as well as $Ba^{2+}$, $Mg^{2+}$ does not give rise to the same level of protection from protease cleavage as does $Ba^{2+}$. Instead, the cleavage pattern obtained with $Mg^{2+}$ more closely resembles that obtained in the absence of divalent metal, suggesting that dimer formation and protease protection are not intimately coupled. The abilities of different divalent metal ions to protect syt II from proteolysis are consistent with previous studies reported for syt I (i.e., $Ca^{2+}$, $Sr^{2+}$, $Ba^{2+}$, and $Pb^{2+}$ protect from cleavage and $Mg^{2+}$ does not; Bouton et al., 2001; Davletov and Sudhof, 1994). In addition, these results support the assertion that the recently reported structure of syt III with $Mg^{2+}$ bound is likely to be in the ''unliganded conformation'' (Sutton et al., 1999).

## CONCLUSION

The high calcium concentrations required for self-association of syt II suggest the oligomerized state of this protein is not a critical intermediate in vesicle fusion at the synaptic cleft. However, the low-affinity calcium sites on syt II may play a critical role in buffering calcium at the presynaptic active zone (Felmy et al., 2003; Trommershèauser et al., 2003). In addition, the high propensity of lead to oligomerize syt II offers a possible molecular explanation for how lead interferes with calcium-evoked neurotransmitter release. Future studies that address the structural origins of the differences in oligomerization propensities between syt I and syt II are warranted.

## SUPPLEMENTAL MATERIALS

An online supplement to this article can be found by visiting BJ Online at http://www.biophysj.org. The supplementary material contains: tables of results of sedimentation equilibrium studies on syt II in the presence of varying concentrations of $Ca^{2+}$, $Ba^{2+}$, $Mg^{2+}$, $Sr^{2+}$, and $Pb^{2+}$; and a table of results of sedimentation equilibrium studies on C2A and C2B domains from syt II in the presence of varying concentrations of $Ca^{2+}$.

We are grateful to Dr. Mitsunori Fukuda for generously providing the cDNA for syt II, to Lydia Finney for her kind help with the mass spectrometer and related software, to Mathew Miller for his help with modeling of syt II, and to Jihong Bai, Edwin Chapman, and Jose Rizo for their helpful discussions. We are also thankful to Angie Ormonde for providing some materials for the AFM experiments and for advice on AFM. Analytical ultracentrifugation data were acquired in the Keck Biophysics Facility at Northwestern University. AFM experiments were conducted in a shared facility of the Catalysis Center at Northwestern University and MALDI-TOF experiments were performed in the Analytical Services Laboratory of the Department of Chemistry at Northwestern University.

This work was supported by a grant from the National Institutes of Health (1 R01 GM58183-01A1). Hilary Arnold Godwin is a recipient of a Camille and Henry Dreyfus New Faculty Award, a Burroughs-Wellcome Fund New Investigator Award in the Toxicological Sciences, a National Science Foundation CAREER Award, a Sloan Research Fellowship, and a Camille Dreyfus Teacher-Scholar Award. Support for Ricardo García was provided by a grant from the National Institutes of Health, Cellular and Molecular Basis of Disease Training Program (T32 GM08061) (http:x.biochem.nwu.edu/Keck/keckmain.html).

## REFERENCES

Bai, J., C. A. Earles, J. L. Lewis, and E. R. Chapman. 2000. Membrane-embedded synaptotagmin penetrates *cis* or *trans* target membranes and clusters via a novel mechanism. *J. Biol. Chem.* 275:25427–25435.

Bollmann, J. H., B. Sakmann, and J. G. Borst. 2000. Calcium sensitivity of glutamate release in a calyx-type terminal. *Science*. 289:953–957.

Bouton, C. M., L. P. Frelin, C. E. Forde, H. A. Godwin, and J. Pevsner. 2001. Synaptotagmin is a molecular target for lead. *J. Neurochem.* 76:1724–1735.

Brose, N., A. G. Petrenko, T. C. Sudhof, and R. Jahn. 1992. Synaptotagmin: a calcium sensor on the synaptic vesicle surface. *Science*. 256:1021–1025.

Brunger, A. T. 2000. Structural insights into the molecular mechanism of $Ca^{2+}$-dependent exocytosis. *Curr. Opin. Neurobiol.* 10:293–302.

Chae, Y. K., F. Abildgaard, E. R. Chapman, and J. L. Markley. 1998. Lipid binding ridge on loops 2 and 3 of the C2A domain of synaptotagmin I as revealed by NMR spectroscopy. *J. Biol. Chem.* 273:25659–25663.

Chapman, E. R., S. An, J. M. Edwardson, and R. Jahn. 1996. A novel function for the second C2 domain of synaptotagmin. *J. Biol. Chem.* 271:5844–5849.

Chapman, E. R., R. C. Desai, A. F. Davis, and C. K. Tornehl. 1998. Delineation of the oligomerization, AP-2 binding, and synprint binding region of the C2B domain of synaptotagmin. *J. Biol. Chem.* 273:32966–32972.

Chapman, E. R., P. I. Hanson, S. An, and R. Jahn. 1995. $Ca^{2+}$ regulates the interaction between synaptotagmin and syntaxin 1. *J. Biol. Chem.* 270:23667–23671.

Chapman, E. R., and R. Jahn. 1994. Calcium-dependent interaction of the cytoplasmic region of synaptotagmin with membranes. *J. Biol. Chem.* 269:5735–5741.

Damer, S. K., and C. E. Creutz. 1996. Calcium-dependent self-association of synaptotagmin I. *J. Neurochem.* 67:1661–1668.

Davis, A. F., J. Bai, D. Fasshauer, M. J. Wolowick, J. L. Lewis, and E. R. Chapman. 1999. Kinetics of synaptotagmin responses to Ca2+ and assembly with the core SNARE complex onto membranes. *Neuron.* 24:363–376. (Published erratum appears in *Neuron* 1999 24:1049).

Davletov, B., O. Perisic, and R. L. Williams. 1998. Calcium-dependent membrane penetration is a hallmark of the C2 domain of cytosolic phospholipase A2 whereas the C2A domain of synaptotagmin binds membranes electrostatically. *J. Biol. Chem.* 273:19093–19096.

Davletov, B., J. M. Sontag, Y. Hata, A. G. Petrenko, E. M. Fykse, R. Jahn, and T. C. Sudhof. 1993. Phosphorylation of synaptotagmin I by casein kinase II. *J. Biol. Chem.* 268:6816–6822.

Davletov, B. A., and T. C. Sudhof. 1993. A single C2 domain from synaptotagmin I is sufficient for high affinity $Ca^{2+}$/phospholipid binding. *J. Biol. Chem.* 268:26386–26390.

Davletov, B. A., and T. C. Sudhof. 1994. $Ca^{2+}$-dependent conformational change in synaptotagmin I. *J. Biol. Chem.* 269:28547–28550.

Desai, R. C., B. Vyas, C. A. Earles, J. T. Littleton, J. A. Kowalchyck, T. F. J. Martin, and E. R. Chapman. 2000. The C2B domain of synaptotagmin is a $Ca^{2+}$-sensing module essential for exocytosis. *J. Cell Biol.* 150:1125–1135.

Edstrom, R. D., M. H. Meinke, X. Yang, R. Yang, V. Elings, and D. F. Evans. 1990. Direct visualization of phosphorylase-phosphorylase

kinase complexes by scanning tunneling and atomic force microscopy. *Biophys. J.* 58:1437–1448.

Elferink, L. A., W. S. Trimble, and R. H. Scheller. 1989. Two vesicle-associated membrane protein genes are differentially expressed in the rat central nervous system. *J. Biol. Chem.* 264:11061–11064.

Felmy, F., E. Neher, and R. Schneggenburger. 2003. Probing the intracellular calcium sensitivity of transmitter release during synaptic facilitation. *Neuron.* 37:801–811.

Fernandez, I., D. Arac, J. Ubach, S. H. Gerber, O. Shin, Y. Gao, R. G. Anderson, T. C. Sudhof, and J. Rizo. 2001. Three-dimensional structure of the synaptotagmin 1 C2B-domain: synaptotagmin 1 as a phospholipid binding machine. *Neuron.* 32:1057–1069.

Fernandez-Chacon, R., A. Konigstorfer, S. H. Gerber, J. García, M. F. Matos, C. F. Stevens, N. Brose, J. Rizo, C. Rosenmund, and T. C. Sudhof. 2001. Synaptotagmin I functions as a calcium regulator of release probability. *Nature.* 410:41–49.

Fon, E. A., and R. H. Edwards. 2001. Molecular mechanisms of neurotransmitter release. *Muscle Nerve.* 24:581–601.

Fukuda, M. 2003a. Molecular cloning and characterization of human, rat, and mouse synaptotagmin XV. *Biochem. Biophys. Res. Commun.* 306: 64–71.

Fukuda, M. 2003b. Molecular cloning, expression, and characterization of a novel class of synaptotagmin (Syt XIV) conserved from *Drosophila* to humans. *J. Biochem.* 133:641–649.

Fukuda, M., E. Kanno, and K. Mikoshiba. 1999. Conserved N-terminal cysteine motif is essential for homo- and heterodimer formation of synaptotagmins III, V, VI, and X. *J. Biol. Chem.* 274:31421–31427.

Fukuda, M., and K. Mikoshiba. 2000a. Calcium-dependent and -independent hetero-oligomerization in the synaptotagmin family. *J. Biochem.* 128:637–645.

Fukuda, M., and K. Mikoshiba. 2000b. Distinct self-oligomerization activities of synaptotagmin family. *J. Biol. Chem.* 275:28180–28185.

Fukuda, M., and K. Mikoshiba. 2000c. Genomic structures of synaptotagmin II protein: comparison of exon-intron organization of the synaptotagmin gene family. *Biochem. Biophys. Res. Commun.* 270: 528–532.

Fukuda, M., and K. Mikoshiba. 2001. Mechanism of the calcium-dependent multimerization of synaptotagmin VII mediated by its first and second C2 domains. *J. Biol. Chem.* 276:27670–27676.

García, R. A., C. J. Bustamante, and N. O. Reich. 1996. Sequence-specific recognition by cytosine $C^5$ and adenine $N^6$ DNA methyltransferases requires different deformations of DNA. *Proc. Natl. Acad. Sci. USA.* 93:7618–7622.

García, R. A., C. E. Forde, and H. A. Godwin. 2000. Calcium triggers an intramolecular association of the C2 domains in synaptotagmin. *Proc. Natl. Acad. Sci. USA.* 97:5883–5888.

Geppert, M., Y. Goda, R. E. Hammer, C. Li, T. W. Rosahi, C. F. Stevens, and T. C. Sudhof. 1994. Synaptotagmin I: a major $Ca^{2+}$ sensor for transmitter release at a central synapse. *Cell.* 79:717–727.

Gerona, R. R. L., E. C. Larsen, J. A. Kowalchyk, and T. F. J. Martin. 2000. The C terminus of SNAP25 is essential for $Ca^{2+}$-dependent binding of synaptotagmin to SNARE complexes. *J. Biol. Chem.* 275:6328–6336.

Kee, Y., and R. H. Scheller. 1996. Localization of synaptotagmin-binding domains on syntaxin. *J. Neurosci.* 16:1975–1981.

Laemmli, U. K. 1970. Cleavage of structural proteins during the assembly of the head of bacteriophage T4. *Nature.* 227:680–685.

Leveque, C., J. A. Boudier, M. Takahashi, and M. Seagar. 2000. Calcium-dependent dissociation of synaptotagmin from synaptic SNARE complexes. *J. Neurochem.* 74:367–374.

Li, C., B. A. Davletov, and T. C. Sudhof. 1995a. Distinct $Ca^{2+}$ and $Sr^{2+}$ binding properties of synaptotagmins. *J. Biol. Chem.* 270:24898–24902.

Li, C., B. Ullrich, J. Z. Zhang, R. G. W. Anderson, N. Brose, and T. C. Sudhof. 1995b. $Ca^{2+}$-dependent and -independent activities of neural and non-neural synaptotagmins. *Nature.* 375:594–599.

Lin, R. C., and R. H. Scheller. 2000. Mechanisms of synaptic vesicle exocytosis. *Ann. Rev. Cell Dev. Biol.* 16:19–49.

Littleton, J. T., J. Bai, B. Vyas, R. Desai, A. E. Baltus, M. B. Garment, S. D. Carlson, B. Ganetzky, and E. R. Chapman. 2001. Synaptotagmin mutants reveal essential functions for the C2B domain in $Ca^{2+}$-triggered fusion and recycling of synaptic vesicles in vivo. *J. Neurosci.* 21:1421–1433.

Littleton, J. T., T. L. Serano, G. M. Rubin, B. Ganetzky, and E. R. Chapman. 1999. Synaptic function modulated by changes in the ratio of synaptotagmin I and IV. *Nature.* 400:757–760.

Manalis, R. S., G. P. Cooper, and S. L. Pomeroy. 1984. Effects of lead on neuromuscular transmission in the frog. *Brain Res.* 294:95–109.

Matos, M. F., J. Rizo, and T. C. Sudhof. 2000. The relation of protein binding to function: what is the significance of munc18 and synaptotagmin binding to syntaxin 1, and where are the corresponding binding sites? *Eur. J. Cell Biol.* 79:377–382.

Misura, K. M. S., A. P. May, and W. I. Wiess. 2000. Protein-protein interactions in intracellular membrane fusion. *Curr. Opin. Struct. Biol.* 10:662–671.

Mochida, S. 2000. Protein-protein interactions in neurotransmitter release. *Neurosci. Res.* 36:175–182.

Mochly-Rosen, D., K. G. Miller, R. H. Scheller, H. Khaner, J. Lopez, and B. Smith. 1992. p65 fragments, homologous to the C2 region of protein kinase C, bind to the intracellular receptors for protein kinase C. *Biochemistry.* 31:8120–8124.

Nalefski, E. A., and J. J. Falke. 1996. The C2 domain calcium-binding motif: structural and functional diversity. *Protein Sci.* 5:2375–2390.

Osborne, S. L., J. Herreros, P. I. Bastiaens, and G. Schiavo. 1999. Calcium-dependent oligomerization of synaptotagmins I and II. Synaptotagmins I and II are localized on the same synaptic vesicle and heterodimerize in the presence of calcium. *J. Biol. Chem.* 274:59–66.

Perin, M. S., V. A. Fried, G. A. Mignery, R. Jahn, and T. C. Sudhof. 1990. Phospholipid binding by a synaptic vesicle protein homologous to the regulatory region of protein kinase C. *Nature.* 345:260–263.

Reist, N. E., J. Buchanan, J. Li, A. DiAntonio, E. M. Buxton, and T. L. Schwarz. 1998. Morphologically docked synaptic vesicles are reduced in synaptotagmin mutants of *Drosophila*. *J. Neurosci.* 18:7662–7673.

Rizo, J., and T. C. Sudhof. 1998. C2-domains, structure and function of a universal $Ca^{2+}$-binding domain. *J. Biol. Chem.* 273:15879–15882.

Schiavo, G., Q. M. Gu, G. D. Prestwich, T. H. Sollner, and J. E. Rothman. 1996. Calcium-dependent switching of the specificity of phosphoinositide binding to synaptotagmin. *Proc. Natl. Acad. Sci. USA.* 93:13327–13332.

Schiavo, G., S. L. Osborne, and J. G. Sgouros. 1998. Synaptotagmins: more isoforms than functions? *Biochem. Biophys. Res. Commun.* 248:1–8.

Schneggenburger, R., and E. Neher. 2000. Intracellular calcium dependence of transmitter release rates at a fast central synapse. *Nature.* 406:889–893.

Schneider, S. W., J. Larmer, R. M. Henderson, and H. Oberleithner. 1998. Molecular weights of individual proteins correlate with molecular volumes measured by atomic force microscopy. *Pfluegers Arch. Eur. J. Physiol.* 435:362–367.

Sehgal, B. U., R. Dunn, L. Hicke, and H. A. Godwin. 2000. High-yield expression and purification of recombinant proteins in bacteria: a versatile vector for glutathione S-transferase fusion proteins containing two protease cleavage sites. *Anal. Biochem.* 281:232–234.

Shao, X., C. Li, I. Fernandez, X. Zhang, T. C. Sudhof, and J. Rizo. 1997. Synaptotagmin-syntaxin interaction: the C2 domain as a $Ca^{2+}$-dependent electrostatic switch. *Neuron.* 18:133–142.

Shin, O. H., J. Rizo, and T. C. Sudhof. 2002. Synaptotagmin function in dense core vesicle exocytosis studied in cracked PC12 cells. *Nat. Neurosci.* 5:649–656.

Smith, S. J., and G. J. Augustine. 1988. Calcium ions, active zones, and synaptic transmitter release. *Trends Neurosci.* 11:458–464.

Sudhof, T. C. 2002. Synaptotagmins: why so many? *J. Biol. Chem.* 277: 7629–7632.

Sugita, S., Y. Hata, and T. Sudhof. 1996. Distinct $Ca^{2+}$-dependent properties of the first and second C2-domains of synaptotagmin I. *J. Biol. Chem.* 271:1262–1265.

Sugita, S., O. H. Shin, W. Han, Y. Lao, and T. C. Sudhof. 2002. Synaptotagmins form a hierarchy of exocytotic $Ca^{2+}$ sensors with distinct $Ca^{2+}$ affinities. *EMBO J.* 21:270–280.

Sugita, S., and T. C. Sudhof. 2000. Specificity of $Ca^{2+}$-dependent protein interactions mediated by the C(2)A domains of synaptotagmins. *Biochemistry.* 39:2940–2949.

Sutton, R. B., B. A. Davletov, A. M. Berghuis, T. C. Sudhof, and S. R. Sprang. 1995. Structure of the first C2 domain of synaptotagmin I: a novel $Ca^{2+}$/phospholipid-binding fold. *Cell.* 80:929–938.

Sutton, R. B., J. A. Ernst, and A. T. Brunger. 1999. Crystal structure of the cytosolic C2A–C2B domains of synaptotagmin III. Implications for $Ca^{+2}$-independent snare complex interaction. *J. Cell Biol.* 147:589–598.

Trommershèauser, J., R. Schneggenburger, A. Zippelius, and E. Neher. 2003. Heterogeneous presynaptic release probabilities: functional relevance for short-term plasticity. *Biophys. J.* 84:1563–1579.

Verona, M., S. Zanotti, T. Schafer, G. Racagni, and M. Popoli. 2000. Changes of synaptotagmin interaction with t-SNARE proteins in vitro after calcium/calmodulin-dependent phosphorylation. *J. Neurochem.* 74:209–221.

von Poser, C., and T. C. Sudhof. 2001. Synaptotagmin 13: structure and expression of a novel synaptotagmin. *Eur. J. Cell Biol.* 80:41–47.

von Poser, C., J. Z. Zhang, C. Mineo, W. Ding, Y. Ying, T. C. Sudhof, and R. G. W. Anderson. 2000. Synaptotagmin regulation of coated pit assembly. *J. Biol. Chem.* 275:30916–30924.

Zhang, J. Z., B. A. Davletov, T. C. Sudhof, and R. G. Anderson. 1994. Synaptotagmin I is a high affinity receptor for clathrin AP-2: implications for membrane recycling. *Cell.* 78:751–760.

Zhang, X., J. Rizo, and T. C. Sudhof. 1998. Mechanism of phospholipid binding by the C2A-domain of synaptotagmin I. *Biochemistry.* 37: 12395–12403.